JOURNAL OF SOLID STATE CHEMISTRY **101**, 237–248 (1992)

Hole Density as Evidenced by XAS and Critical Temperature in the $TlBa_2Ca_{1-x}Nd_xCu_2O_{7-\delta}$ Series

N. MERRIEN, F. STUDER, C. MARTIN, A. MAIGNAN, C. MICHEL, AND B. RAVEAU

Laboratoire CRISMAT–ISMRA, Université de Caen, Boulevard du Maréchal Juin, 14050 Caen Cedex, France

AND A.-M. FLANK

Lure, Bât. 209d, 91405 Orsay Cedex, France

Received December 20, 1991; in revised form April 28, 1992; accepted April 30, 1992

To estimate the variations of the doping hole density in a series of thallium cuprates, $TlBa_2Ca_{1-x}Nd_xCu_2O_{7-\delta}$ with the substitution amount x, we used XAS at the copper L_3-edge. The spectra were recorded on powder samples with the total electron yield method. From the simulations of the spectra with two pseudo-Voigt functions, the $|3d^9\underline{L}>$ relative intensity, with respect to the $|3d^9>$ one, has been calculated and compared to the variations of T_c's and to the copper formal charge deduced from previous neutron diffraction experiments. A correlation between the doping hole density in the $[CuO_2]_\infty$ planes, $n_h(x, y)$, and T_c's has been clearly established. The difference between the copper formal charge as deduced from neutron diffraction and the equivalent one deduced from our experiments has been assigned to extra holes likely located in the $2p_z$ orbitals of the apical oxygen of the copper square pyramids. © 1992 Academic Press, Inc.

I. Introduction

Comparison of the two series of high T_c superconductors $Tl_2Ba_2Ca_{m-1}Cu_mO_{2m+4}$ (labeled "Tl_2") and $TlBa_2Ca_{m-1}Cu_mO_{2m+3}$ (labeled "Tl") raises the question of the influence of the Cu(III) content upon the superconducting properties of these compounds. Indeed the first series should contain no Cu(III), whereas the second series should present very high Cu(III) contents, especially for the first member, $TlBa_2CaCu_2O_7$, if one takes into account the stoichiometric formula. Several hypotheses

[1] In most of these oxides, the oxygen content is only determined by chemical methods which is a volumetric analysis capable of determining the total amount of active oxygen (see for instance Parantham *et al., J. Solid State Chem.* **87**, 479, 1990). However, it cannot differentiate the species, especially in the case of many mixed-valence elements being present simultaneously in a single phase, so that it is questionable, and moreover the structure determination is not performed on the sample studied for superconductivity. Consequently, it is not possible to draw out conclusions about the role of oxygen and the density of carriers in the $[Cu-O_2]_\infty$ planes necessary for superconductivity. Conversely, X-ray absorption spectroscopy deals with the electronic structure and is able to determine the hole density close to the Fermi level of one specific element inside a complex structure.

0022-4596/92 $5.00

have been put forward to explain superconductivity in these phases such as, for instance, the role of the hole reservoir of the $[TlO]_\infty$ layers and the possible excess oxygen in the Tl_2 compounds and oxygen deficiency in the Tl oxides.[1]

XAS has been shown to be a valuable tool to estimate the formal valence and the electronic structure of elements in superconducting oxides (*1–6*). The XAS studies of bismuth (*7, 8*) and thallium layered cuprates (*9, 10*) have been interpreted on the basis of a partial reduced valence of the Tl and Bi cations due not to the formation of stable reduced valence states Tl(I) or Bi(I), but more likely to the delocalization of electrons on an hybridized band made of 6*s*, 6*p*, and 6*d* levels in the Bi–O or Tl–O planes.

For the interpretation of the copper L_3-edge spectra, we agree with the charge transfer model generally used to describe the spectroscopic properties of the superconducting copper oxides: this situation occurs when the ligand-to-metal charge transfer energy $\Delta = E(d^{n+1}L) - E(d^n)$ (the energy required for $d^n \rightarrow d^{n+1}\underline{L}$ transition) is smaller than the intra-atomic Coulomb energy U. Undoped, the cuprates are insulators of the charge transfer type. In other words the full valence band originates essentially from 2*p* oxygen orbitals but contains 3*d* character. The first empty band above the Fermi level is based on $3d_{x^2-y^2}$ orbitals of Cu but has a partial 2*p* character due to covalency. The Cu(III) term is used only to illustrate the charge balance in the chemical formula and represents a simplified and abbreviated concept to image the cation Cu(II), described as an admixture of configurations ($\alpha|3d^9> + \beta|3d^{10}\underline{L}>$ with $\alpha^2 + \beta^2 = 1$) in the presence of itinerant 2*p* holes. The $\underline{L}$ ligand hole is also an oxygen 2*p* hole but without any itinerant capability.

By doping, a hole impuritylike band is formed at the bottom of the gap, which finally merges with the valence band to build a partially filled conduction band. Thus the stable electronic configuration for these doping holes is the $|3d^9\underline{L}>$ one, and the $|3d^8>$ configuration appears only at higher energy as shown by Bianconi *et al.* (*31*). Moreover, it has been found that α^2 increases with hole doping.

To directly check the hole density in the $[CuO_2]_\infty$ planes, one can use XAS either at the oxygen K edge or at the Cu L_3 edge. Direct observations of $La_{2-x}Sr_xCuO_{4-x/2+\delta}$, "123" phases, and $Bi_2Sr_2CaCu_2O_{8+\delta}$ compounds at the oxygen K edge have shown the oxygen 2*p* character of the conduction band, the presence of a high density of holes, and the strong anisotropy of the hole symmetry in the layered cuprates (*11–14*). The Cu L_3-edge spectroscopy is also a tool of choice to probe the filling of the *d* band (*15, 16*). The presence of holes is clearly evidenced by an absorption peak due to the $|3d^9\underline{L}>$ (hole doping) configuration. But the problem here comes from the polarization of this transition as observed on single crystals of $YBa_2Cu_3O_7$ and $Bi_2Sr_2CaCu_2O_{8+\delta}$ superconductors.

In this respect, the 1212 series exhibits an interesting behavior since the critical temperature of the oxide $TlBa_2CaCu_2O_7$ (*17–19*) was shown to increase from about 50 to 65 K by annealing in an inert atmosphere. This influence of the oxygen content, i.e., of the modification of the hole carrier density upon T_c's was shown recently by hydrogen–argon annealing of various thallium cuprates (*20, 21*) for which the critical temperature could be increased in a dramatic way.

Another remarkable feature of the 1212 series deals with the fact that the complete replacement of calcium by yttrium or neodymium allows pure nonsuperconducting phases to be synthesized (*22, 23*). Indeed, this absence of superconductivity in $TlBa_2NdCu_2O_7$ needs to be compared to the existence of superconductivity at high temperature in $Tl_2Ba_2CaCu_2O_8$ which exhibits, from its formula, the same charge balance,

i.e., "Tl(III)–Cu(II)." More recently, it was shown that the partial replacement of calcium by rare earth elements (Nd, Y, Gd) in $TlBa_2CaCu_2O_7$ allowed T_c to be increased up to 100 K (*24*).

A neutron diffraction study was performed on the $TlBa_2Ca_{1-x}Nd_xCu_2O_{7-\delta}$ compounds to understand these phenomena (*25*); the authors have determined precisely the oxygen content. As a result, the copper formal charges have been indirectly determined and shown to decrease from $x = 0.2$ to $x = 1$ when T_c's decreased from 100 K to no superconductivity. Moreover a new relation between Cu–O apical distances in the CuO_5 square pyramidal layers and T_c's has been found for oxides belonging to a same solid solution: the larger the Cu–O apical distances, the larger the critical temperatures.

In this work, we will present and discuss X-ray absorption spectroscopy of the thallium cuprates series $TlBa_2Ca_{1-x}Nd_xCu_2O_{7-\delta}$ ($0.2 \leq x \leq 1$). The samples used in this study were the same as those used for X-ray diffraction characterization, magnetic susceptibility measurements, and neutron diffraction so that the oxygen content and the superconducting properties were well known. In the present study, the Cu L_3-edge spectra of the $TlBa_2Ca_{1-x}Nd_xCu_2O_{7-\delta}$ series will be simulated in order to get quantitative information about the hole density on the copper sites and to compare it with the copper formal charges deduced from neutron diffraction and with the variations of critical temperature.

II. Experimental

The oxides Tl_2O_3, BaO_2, CuO, CaO, and Nd_2O_3 were mixed in the adequate ratios. The mixtures were pressed into bars of 4 mm diameter × 50 mm length (about 2 g weight) and heated in evacuated quartz ampoules (heating rate, 150°C/hr; reaction time, 24 hr at 950°C; cooling rate, 8°C/hr from 950 to 600°C and then furnace cooled).

Neodymium, Nd_2CuO_4, and lanthanum cuprates, La_2CuO_4 (reference compounds for the Cu(II) formal valence state), were prepared from the oxides, Nd_2O_3, La_2O_3, and CuO, mixed, and heated in air in platinum crucibles at 1100°C for Nd_2CuO_4.

$La_2Cu_{0.5}Li_{0.5}O_{4-\delta}$ (reference compound for the Cu(III) formal valence state) was synthesized from a mixture of the oxides La_2O_3 and CuO and of lithium carbonate Li_2CO_3 according to the work of Attfield and Férey (*26*). The preparation was pelletized, heated in flowing oxygen at 900°C for 12 hr, and cooled to room temperature at the rate of 50°C/hr. TGA analysis could not be performed on this sample due to the possibility of lithium loss during the reduction. Iodometric titration confirmed the presence of trivalent copper and led to a δ value close to 0.04.

These materials were checked by X-ray and electron diffraction for purity and defects density. Superconducting properties were studied by susceptibility measurements. Structure determinations and physical properties of these compounds have been published elsewhere (*17, 22, 25, 27, 28*).

All the XAS spectra at the L_3 edge of copper were recorded at room temperature on powder samples by a total electron yield method. The experiments were performed at LURE (Orsay) using the synchrotron radiation from the super-ACO ring operated at 800 MeV with a typical current of 250 mA. Samples were ground and sieved homogeneously on a sticky band supported by an aluminum sample holder. Electrical contacts were realized by silver paste dots. The X-rays were monochromatized by two beryl crystals ($10\underline{1}0$) and the ejected electrons from the samples detected by a channeltron with an axis perpendicular to the beam line. The energy scale was then positioned with respect to the $|3d^9>$ peak of

CuO at 931.2 eV. The experimental energy resolution was estimated to be better than 0.3 eV, whereas the reproducibility of the energy position of the spectral features is close to 0.05 eV. The width of the core hole has been measured to be 0.56 eV at the L_3 edge (*29*). The usual thickness of the probed upper layer of the samples is about 200 Å in the total electron yield method.

The top of the $|3d^9>$ transitions for all the compounds has been set to a common value chosen arbitrarily. In order to obtain the relative intensities of the transitions, the spectra have been least-squares fitted by a combination of Gaussian and Lorentzian shapes using a program written by Rodriguez to fit neutron diffraction line profiles. The initial program has been modified to take into account the specificities of X-ray absorption data and to introduce a linewidth per peak as a fitted parameter.

III. Results

Formal Valence States

Cu(II). Copper L_3-edge spectra of cuprates, Nd_2CuO_4, and nonsuperconducting La_2CuO_4, taken as references for Cu(II) valence states in previous papers (*9, 10*), are shown Figs. 1a and 1b. They are characterized by one peak centered around 931.2 eV; energies and linewidths (deduced from the fits) are reported in Table I. Fitted curves are shown on the experimental data (Figs. 1a and 1b). The single peak corresponds to the transition $|2p_{3/2}3d^9> \rightarrow |2p3d^{10}>$, giving rise to the copper final state $[1s^22s^22p^53s^23p^63d^{10}4s^04p^0]$.

Another peak of low intensity appears around 938 eV in these reference spectra; it should correspond to the $|2p_{3/2}4s^0> \rightarrow |2p4s^1>$ transition which presents a much lower cross section than the first one. Indeed recent XANES simulations have shown that this second peak results from electronic transition to hybridized levels built on 4*s*, 4*p*, and 3*d* copper orbitals (*30*).

Cu(III). The K_2NiF_4-type compound $La_2Li_{0.5}Cu_{0.5}O_{4-\delta}$ has been chosen as a reference for the Cu(III) valence state since it is stable in air over long periods. From the iodometric titration, δ was measured to be 0.04 and thus the copper formal charge must be +2.84, assuming adequate lithium stoichiometry. The Cu L_3 edge of this compound is shown in Fig. 2 together with the fitted curve. Two peaks are clearly visible due to a large energy difference; the intensity of the second peak at $E_1 = 933.45$ eV (see Table I) is quite a bit larger than the other one at $E_0 = 931.1$, keeping the same (HWHM) linewidths. The energy of the first peak is close to the values found for the Cu(II) references, Nd_2CuO_4 and La_2CuO_4, and thus the corresponding transition must be $|2p_{3/2}3d^9> \rightarrow |2p3d^{10}>$, attesting to the presence of Cu(II) valence state in small amounts.

For the second peak, the core electron can be transferred to two possible initial electronic configurations $|3d^8>$ and $|3d^9\underline{L}>$, the $|3d^{10}\underline{L}^2>$ being unaccessible at the Cu L_3 edge due to the selection rules. From previous XPS measurements made by Bianconi *et al.* (*31*), it has been shown that the $|3d^8>$ configuration has a very small transition probability such that the main peak appears very likely to be due to transitions to the $|3d^9\underline{L}>$. Indeed, this compound is an insulator presenting an ordering in the $[(Cu, Li)O]_\infty$ planes and exhibiting a diamagnetic behavior likely due to an antiferromagnetic coupling between the *d* hole and the 2*p* hole. From the intensities of both peaks I_0 and I_1 (Table I), one can deduce a mean density of holes per copper

$$n_h = I_{|3d^9\underline{L}>}/I_{|3d^9\underline{L}>} + I_{|3d^9>} = 0.85$$

in good agreement with the chemical analysis. It is worth noting here that, in the charge transfer model, the doping hole density in the $2p_{x,y}$ oxygen band should only be 0.425 due to the small copper concentration in this cuprate.

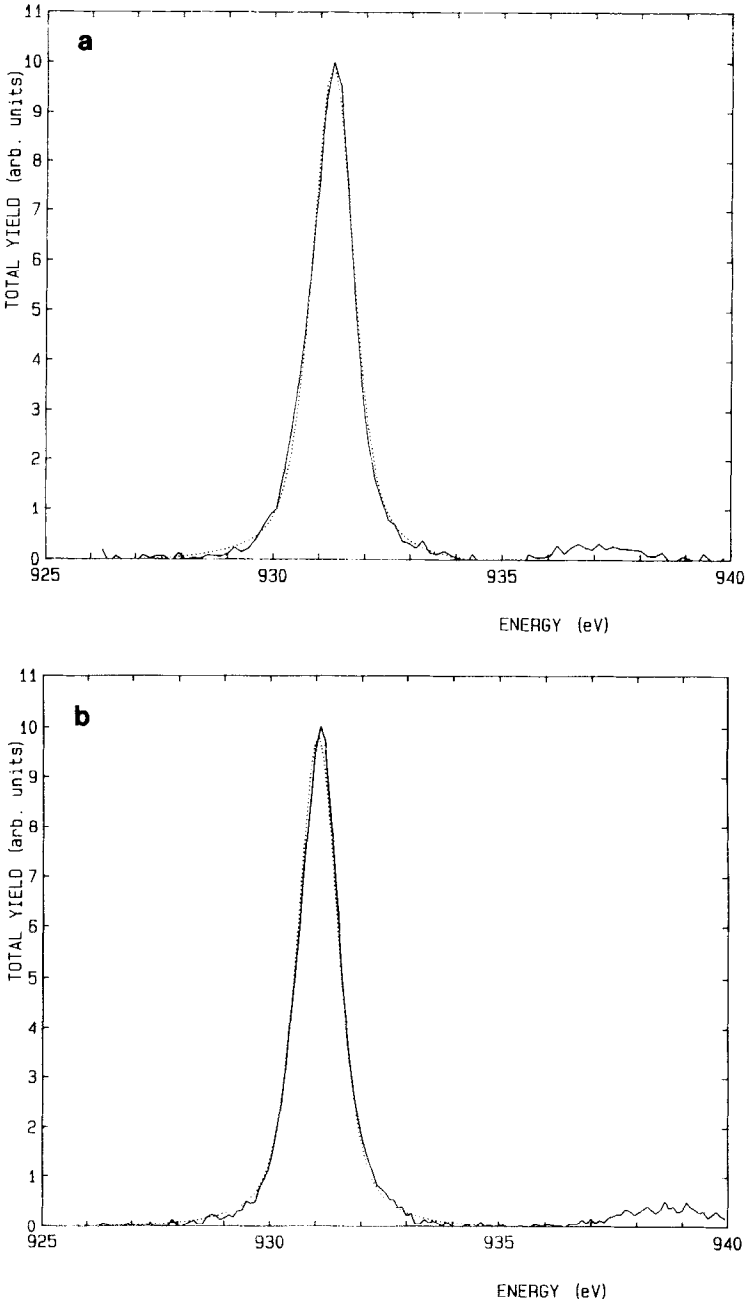

FIG. 1. Copper L_3 edge of reference compounds for the Cu(II) valence state, exhibiting a single peak corresponding to the transition $|2p_{3/2}3d^9> \rightarrow |\underline{2p}3d^{10}>$ due to covalent holes. (a) Nd_2CuO_4: (——) experimental curve; (···) fit. (b) La_2CuO_4: (——) experimental curve; (···) fit.

TABLE I

SIMULATION PARAMETERS OF THE COPPER L_3 EDGES FOR REFERENCES AND SUPERCONDUCTING CUPRATES OF THE $TlBa_2Ca_{1-x}Nd_xCu_2O_{7-\delta}$ SERIES

Compounds		$\|3d^9>$	$\|3d^9\underline{L}>$	$n_h = I/(I + Io)$	$n_{x,y}$	Neutron diffraction (9)
Nd_2CuO_4	E	931.3	[a]	[a]	[a]	[b]
	Γ	0.54				
La_2CuO_4	E	931.1	[a]	[a]	[a]	[b]
	Γ	0.53				
$La_2Li_{0.5}Cu_{0.5}O_4$	E	931.1	933.45	0.84	0.84	[b]
	Γ	0.46	0.47		0.16	
$TlBa_2Ca_{0.8}Nd_{0.2}Cu_2O_{6.86}$	E	931.1	932.4	0.14	0.21	$q_{Cu} = 2.32$
	Γ	0.67	0.8		0.14	$O_{6.86}$ $T_c = 98$ K
$TlBa_2Ca_{0.7}Nd_{0.3}Cu_2O_{7-\delta}$	E	931.1	932.3	0.12	0.18	[b]
	Γ	0.63	0.8		0.12	$T_c = 90$ K
$TlBa_2Ca_{0.6}Nd_{0.4}Cu_2O_{7-\delta}$	E	931.1	932.5	0.10	0.15	[b]
	Γ	0.6	0.8		0.09	$T_c = 60$ K
$TlBa_2Ca_{0.5}Nd_{0.5}Cu_2O_{6.86}$	E	931.1	932.6	0.08	0.12	$q_{Cu} = 2.18$
	Γ	0.62	0.8			$O_{6.86}$ $T_c = 40$ K
$TlBa_2Ca_{0.2}Nd_{0.8}Cu_2O_{7-\delta}$	E	931.1	[a]	<0.06	<0.06	[b]
	Γ	0.57				$T_c = 0$ K
$TlBa_2NdCu_2O_7$	E	931.1	[a]	0	0	$q_{Cu} = 2$
	Γ	0.55				$O_{6.96}$ $T_c = 0$ K

Note. In order to properly compare the $|3d^9\underline{L}>$ line intensities, the linewidth of this transition has been kept constant and fixed to 0.8 eV. E and Γ are, respectively, the energy and linewidth of the lines.

[a] Not detectable $|3d^9\underline{L}>$ line.

[b] Neutron diffraction spectra not recorded.

Thallium Layered Cuprates

Five compositions of the solid solution $TlBa_2Ca_{1-x}Nd_xCu_2O_7$, corresponding to $x = 0.2$, $x = 0.3$, $x = 0.4$, $x = 0.5$, $x = 0.8$, and $x = 1$, have been studied by X-ray absorption spectroscopy at the Cu L_3 edge. A neutron diffraction study (*25*) of some members of the series ($x = 0.2$, $x = 0.5$, and $x = 1$) has shown that these superconducting oxides became oxygen deficient as the calcium content increases and that the corresponding copper formal charges increase as well as T_c's.

The idealized structure of these 1212-type cuprates is shown in Fig. 3a, whereas magnetic susceptibilities for the $x = 0.2$, $x = 0.3$, $x = 0.4$, and $x = 0.5$ compounds are plotted in Fig. 3b. The latter curves show clearly the decrease of T_c's and diamagnetic volumes with increasing substitution rate.

With total electron yield curves (Fig. 4) at the copper L_3 edge, one can clearly observe the increase of the $|3d^9\underline{L}>$ line intensity as the calcium content increases. For the determination of the line intensities, we have simulated the spectra with two lines taking the energies, linewidths, and intensities as fitting parameters as well as the admixture of Lorentzian and Gaussian shapes to take into account the distortion of the experimental line. For example, the spectrum of the thallium cuprate $TlBa_2Ca_{0.8}Nd_{0.2}O_{6.86}$ (Fig. 5) shows the agreement between experimental and simulated curves and the intensity distribution between both lines. The results of the simulation (Table I) show that the energy shift of $|3d^9\underline{L}>$ ($\varepsilon = E_0 - E_1 = 1.5 \pm 0.1$ eV) is constant and smaller than that in the $La_2Li_{0.5}Cu_{0.5}O_{4-x}$ compound ($\varepsilon = 2.3$ eV).

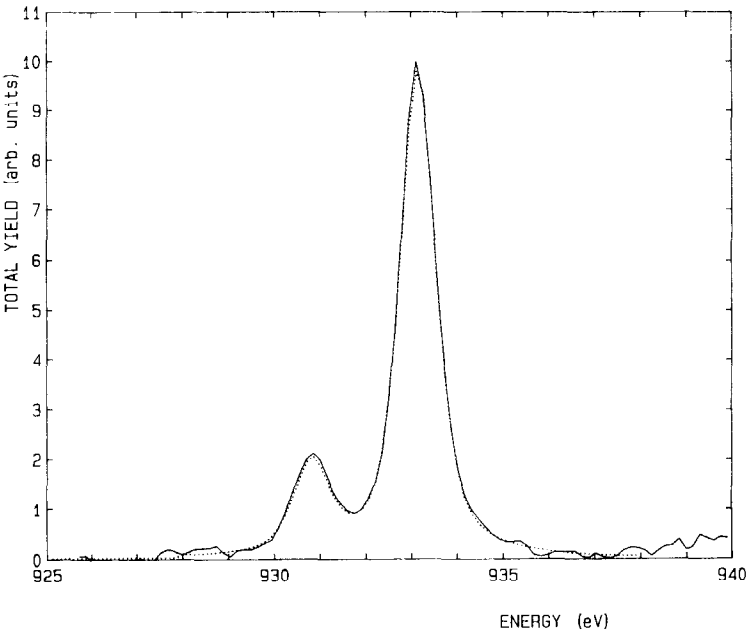

FIG. 2. Copper L_3 edge of the $La_2Li_{0.5}Cu_{0.5}O_{3.96}$ reference compound for the Cu(III) formal valence state, showing two peaks at 931.1 and 933.45 eV, corresponding to $|2p_{3/2}3d^9> \rightarrow |\underline{2p}3d^{10}>$ (covalent holes) and $|2p_{3/2}3d^9\underline{L}> \rightarrow |\underline{2p}3d^{10}\underline{L}>$ (doping holes) transitions, respectively.

In the $TlBa_2Ca_{1-x}Nd_xCu_2O_{7-\delta}$ series, the linewidths of the $|3d^9\underline{L}>$ line appear to be always slightly larger than the $|3d^9>$ one, and this result can probably be related to the random distribution of oxygen vacancies and thus to the distribution of electronic state energies in the hole impurity band following a model described by Tolentino *et al.* (*32*). These $|3d^9\underline{L}>$ linewidths have been kept constant in all the simulations in order to be free of the influence of these parameter fluctuations on the line intensities.

IV. Discussion

In agreement with the neutron diffraction data, which allow one to calculate a copper formal charge close to 2+ in the $TlBa_2NdCu_2O_7$ compound, no density of doping holes could be detected on the copper L_3-edge spectrum (Fig. 4), which shows only the main $|3d^9>$ line due to covalent holes. The absence of the $|3d^9\underline{L}>$ line shows that no doping holes are present in the $[CuO_2]_\infty$ planes of the compound; taking into account the resolution of the experiment ($\Delta E \approx 0.8$ eV), the absolute error on such a determination can be estimated to be $\pm 3\%$.

Increasing the calcium content, one can see (Fig. 4) the increase of the $|3d^9\underline{L}>$ contribution since $x = 0.5$. The absence of any enlargement of the high energy shoulder for the $x = 0.8$ compound shows that the density of doping holes for this composition should be less than 6%. From $x = 0.5$ to $x = 0.2$, the calculated densities of doping holes n_h increase with the calcium content at the same time as T_c's increase (Table I). Unfortunately, no pure phase corresponding to $x = 0$ could be synthesized so that the variation of T_c for larger doping hole densities could not be measured in this series. But looking now at the copper formal

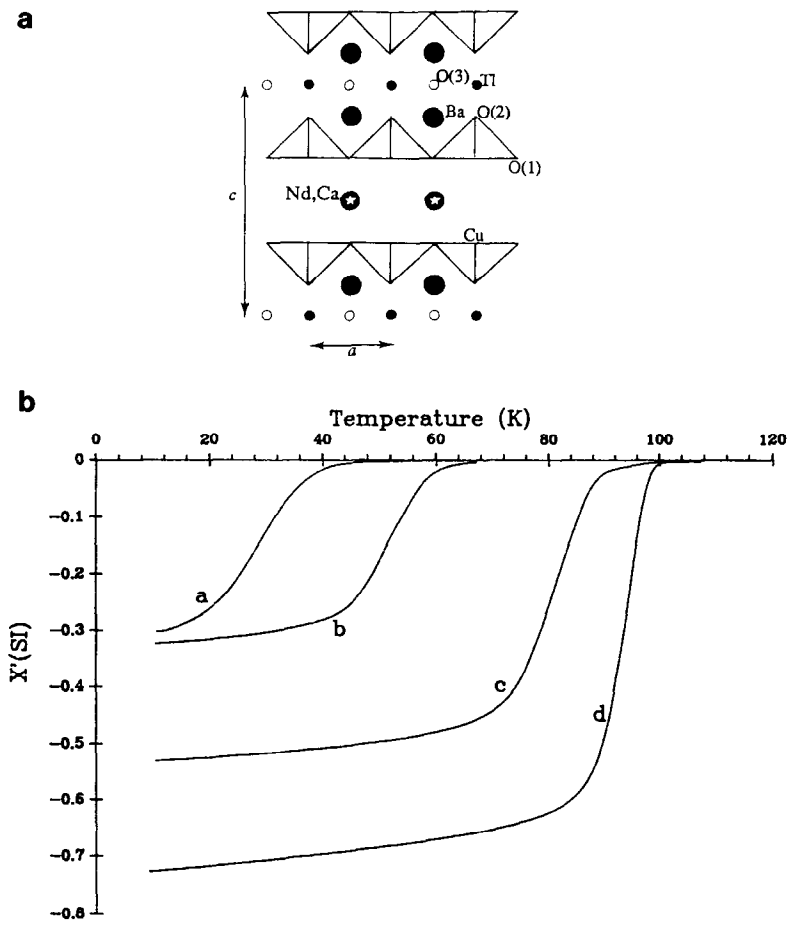

FIG. 3. (a) Structure of the "1212" thallium cuprates family. (b) AC susceptibility $\chi'(T)$ for four compounds of the series $TlBa_2Ca_{1-x}Nd_xCu_2O_{7-\delta}$, showing the simultaneous decrease of both T_c's and diamagnetic volumes. (a) $x = 0.5$; (b) $x = 0.4$; (c) $x = 0.3$; (d) $x = 0.2$.

charges, calculated from the oxygen contents due to the neutron diffraction experiment, for the two compositions $x = 0.2$ and $x = 0.5$, where they are larger than 2, one can see that they are quite a bit larger than the corresponding densities of doping holes observed in the copper L_3-edge spectra.

To explain such a difference, one can think first of the anisotropic distribution of the hole carriers in the very anisotropic structure of the layered cuprates. In the bismuth layered cuprate of the 2212 type, it has been shown by EELS (*14*) at the oxygen K edge that the doping holes are introduced only in the oxygen $2p_{x,y}$ orbitals and are completely absent from the $2p_z$ orbitals. That result is in agreement with the copper L_3-edge spectra realized on thin films or single crystals by Bianconi *et al.* (*15, 16*). With the electric field of the X-ray beam in the (*a, b*) plane of the structure, the $|3d^9\underline{L}>$ transition appears clearly on the high energy side of the main peak, whereas, with the electric field nearly parallel ($\pm 15°$) to the *c* axis of the structure, the $|3d^9\underline{L}>$ does not appear any more and the total intensity is

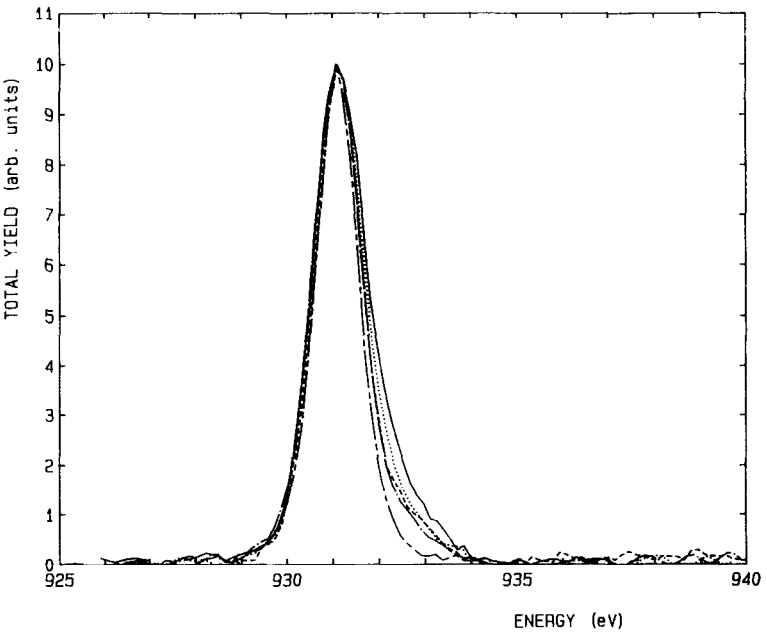

FIG. 4. Copper L_3 edge for five substitution amounts x in the $TlBa_2Ca_{1-x}Nd_xCu_2O_{7-\delta}$ series, showing the increase of the $|2p_{3/2}3d^9\underline{L}> \rightarrow |2p3d^{10}\underline{L}>$ transition intensity with decreasing x. (——) $x = 0.2$; (···) $x = 0.3$; (---) $x = 0.4$; (-·-) $x = 0.5$; (—··—) $x = 1$.

reduced to 20% of the former. Thus, in the bismuth cuprates, with the electrical field direction at an angle θ from the (a, b) plane, the $|3d^9\underline{L}>$ intensities are $I_{|3d^9\underline{L}>}(\theta) = I_{|3d^9\underline{L}>}(0°) \cdot \cos^2(\theta)$ according to the dipole approximation. These results would suggest that the essentials of the doping holes are concentrated in the (a, b) plane in electronic levels based on the oxygen $2p_{x,y}$ orbitals in the bismuth cuprates. Such an electronic configuration can be thought of also for thallium cuprates which present the same type of lamellar structure. Furthermore, in powder samples where the grains are randomly distributed, the $|3d^9\underline{L}>$ relative intensity can be calculated from both contributions $I_{\parallel}$ along the c axis and $I_{\perp}$ perpendicular to the c axis using the angle θ between the electrical field of the incident beam and the (a, b) plane of the structure: $I = I_{\parallel} \cdot \cos(\theta) + I_{\perp} \cdot \sin(\theta)$ with $I_{\parallel} = I_z$ and $I_{\perp} = I_x = I_y$. The isotropic condition leads to $\sin^2(\theta) = \frac{1}{3}$ and $\cos^2(\theta) = \frac{2}{3}$ as a possible solution and thus to $\theta = 35.2°$. Then the powder spectrum must correspond to the spectrum of an oriented sample with the electric field at 35° from the (a, b) plane: $I_{|3d^9\underline{L}>} = I_{|3d^9\underline{L}(x,y)>} \cdot \cos^2(35°)$. Owing to this correction, the final doping hole content per copper $n_{x,y} = I_{|3d^9\underline{L}(x,y)>}/(I_{|3d^9\underline{L}(x,y)>} + I_{|3d^9>})$ in the $[CuO_2]_\infty$ planes of the $TlBa_2Ca_{1-x}Nd_xCu_2O_{7-\delta}$ can be calculated (Table I) and compared to the formal charges derived from the oxygen stoichiometry measured by neutron diffraction. For the substitution rates $x = 0.2$ and $x = 0.5$, one can see that the XAS results are systematically below those deduced from neutron diffraction. The difference, which can be estimated to be one-third of the total copper formal charge, can be due to some extra holes located, for instance, on the $2p_z$ level of the apical oxygen of the CuO_5 pyramid located in the $[Ba–O]_\infty$ planes. Indeed recent EELS work on a $Tl_2Ba_2CaCu_2O_{8+\delta}$

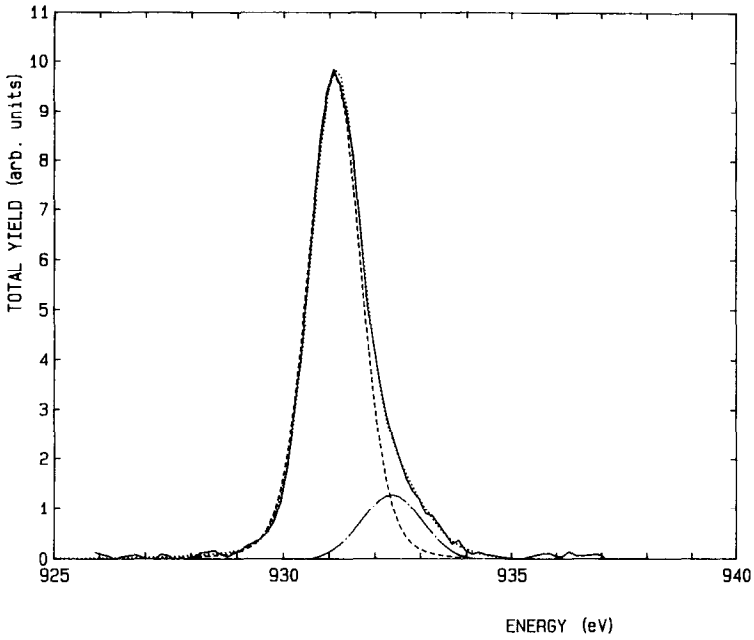

FIG. 5. Copper L_3 edge of the $TlBa_2Ca_{0.8}Nd_{0.2}Cu_2O_{6.86}$ compound and simulation with two peaks due to $|2p_{3/2}3d^9> \rightarrow |2p3d^{10}>$ and $|2p_{3/2}3d^9\underline{L}> \rightarrow |2p3d^{10}\underline{L}>$ transitions, respectively. (——) Experimental curve; (···) total fit; (---) $|3d^9>$ simulated peak; (–·–) $|3d^9\underline{L}>$ simulated peak.

single crystal (*33*) has shown the existence of a large amount of doping holes in the oxygen $2p_z$ orbital at the oxygen K edge, whereas no significant change could be detected by XAS at the Cu L_3 edge. This result needs to be confirmed on other single crystals and oriented thin films but it corresponds to the first observation of holes out of the $[CuO_2]_\infty$ plane in the layered cuprates.

To explain the anisotropy of the $|3d^9\underline{L}>$ line in the thallium layered cuprates, one must deal with the amount of covalent overlapping between the copper $3d_{z^2-r^2}$ orbital and the $2p_z$ orbital of the apical oxygen. The latter interaction depends strongly on the Cu–O apical distance in the dipolar approximation; most X-ray and neutron diffraction structure determinations (*25*, *34*) have shown that the Cu–O distances in the (*a*, *b*) plane ($d_{Cu-O} \cong 1.9$ Å) are much smaller than the apical ones ($d_{Cu-O} \cong 2.7$ Å) in thallium cuprates (*25*). This result suggests a negligible overlap of copper and oxygen orbitals along the *c* axis of the $TlBa_2Ca_{1-x}Nd_xCu_2O_{7-\delta}$ structure and consequently a strong localization of some doping holes in the oxygen $2p_z$ orbitals.

V. Conclusion

We used X-ray absorption spectroscopy at the Cu L_3 edge on thallium cuprates $TlBa_2Ca_{1-x}Nd_xCu_2O_{7-\delta}$ ($0.2 \leq x \leq 1$) in order to investigate the hole density in the copper planes and to correlate it with the copper formal charges deduced from neutron diffraction measurements. The intensities of the $|3d^9\underline{L}>$ electronic configuration, i.e., the doping hole densities, have been correlated to the critical temperatures and decrease when neodymium content increase. Comparing calculated estimation of

doping holes with the copper formal charge, we conclude that the observed difference can be due to extra holes located on the $2p_z$ level of the apical oxygen of the CuO_5 pyramid.

References

1. A. Bianconi, J. Budnick, A. M. Flank, A. Fontaine, P. Lagarde, A. Marcelli, H. Tolentino, B. Chamberland, G. Demazeau, C. Michel, and B. Raveau, *Phys. Lett. A* **127,** 285 (1988).
2. E. E. Alp, G. K. Shenoy, D. G. Hinks, D. W. Capone, II, L. Soderholm, H. B. Schuttler, J. Guo, D. Ellis, P. A. Montano, and M. Ramanathan, *Phys. Rev. B* **35**(13), 7199 (1987).
3. F. Baudelet, G. Collin, E. Dartyge, A. Fontaine, J. P. Kappler, G. Krill, J. P. Itie, J. Jegoudez, M. Maurer, Ph. Monod, A. Revcolevski, H. Tolentino, G. Tourillon, and M. Verdaguer, *Z. Phys. B* **69,** 141 (1988).
4. A. Bianconi, A. Clozza, A. Castellano, S. Dellalonga, M. De Santis, A. Dicicco, K. Garg, P. Delocv, A. Gargano, R. Giorgi, P. Lagarde, A. M. Flank, and A. Marcelli, *J. Phys. C* **9,** 1179 (1988).
5. T. Gourieux, G. Krill, M. Maurier, M. F. Ravet, A. Menny, H. Tolentino, and A. Fontaine, *Phys. Rev. B* **37,** 7516 (1988).
6. H. Tolentino, A. Fontaine, A. M. Flank, P. Lagarde, J. Y. Henry, J. Rossat-Mignod, T. Gourieux, G. Krill, and F. Studer, in "IWEPS, 90" (I. Fink, Ed.), Springer Series of Solid State Sciences, Springer, New York (in press).
7. B. Raveau, C. Michel, M. Hervieu, J. Provost, and F. Studer, "Earlier and Recent Aspects of Superconductivity" (J. G. Bednorz and K. A. Müller, Eds.), pp. 66–95, Solid State Sciences 90.
8. R. Retoux, F. Studer, C. Michel, B. Raveau, A. Fontaine, and E. Dartyge, *Phys. Rev. B* **41,** 193 (1990).
9. F. Studer, D. Bourgault, C. Martin, R. Retoux, C. Michel, and B. Raveau, *Physica C* **159,** 609 (1990).
10. F. Studer, N. Merrien, C. Martin, C. Michel, and B. Raveau, *Physica C* **178,** 324 (1991).
11. P. Kuiper, G. Kruizinga, J. Ghijsen, G. A. Sawatzky, and H. Verweij, *Phys. Rev. Lett.* **62**(2), 221 (1989).
12. T. Chen, F. Sette, Y. Ma, M. S. Hybertsen, E. B. Stechel, W. M. C. Foulkes, M. Schluter, S.-W. Cheong, A. S. Cooper, L. W. Rupp, B. Batlogg, Y. L. Soo, Z. H. Ming, A. Krol, and Y. H. Kao, *Phys. Rev. Lett.* **66**(1), 104 (1991).
13. J. Fink, J. Pflüger, Th. Müller-Heinzerling, N. Nücker, B. Scheerer, H. Romberg, M. Alexander, R. Manzke, T. Buslaps, R. Claessen, and M. Skibowski, in "Proceedings of the International School of Material Science and Technology, July 1989, Erice" (K. A. Müller and G. Berdnoz, Eds.), p. 377.
14. J. Fink, N. Nücker, H. Romberg, M. Alexander, and P. Adelman, in "Proceedings of a NATO Science Forum, Biarritz, France, Sept 16–21, 1990."
15. A. Bianconi, M. De Santis, A. Di Cicco, A. M. Flank, A. Fontaine, P. Lagarde, H. Katayama-Yoshida, A. Kotani, and A. Marcelli, *Phys. Rev. B* **38**(10), 7196 (1988).
16. A. M. Flank, P. Lagarde, A. Bianconi, P. Castrucci, A. Fabrizi, M. Pompa, H. Katayama-Yoshida, and G. Calestani, *Physica Scripta* **41,** 901 (1990).
17. M. Hervieu, A. Maignan, C. Martin, C. Michel, J. Provost, and B. Raveau, *J. Solid State Chem.* **75,** 212 (1988).
18. S. Parkin, V. Lee, A. I. Nazzal, R. Savoy, T. C. Huang, G. Gurman, and R. Beyers, *Phys. Rev. B* **38,** 6531 (1988).
19. B. Morosin, D. S. Ginley, P. F. Hlava, M. J. Carr, R. J. Baughman, J. E. Schirber, E. S. Venturini, and J. F. Kwak, *Physica C* **152,** 413 (1988).
20. C. Martin, A. Maignan, J. Provost, C. Michel, M. Hervieu, R. Tournier, and B. Raveau, *Physica C* **168,** 8 (1990).
21. A. Maignan, C. Martin, M. Huve, J. Provost, M. Hervieu, C. Michel, and B. Raveau, *Physica C* **170,** 350 (1990).
22. C. Martin, D. Bourgault, C. Michel, M. Hervieu, and B. Raveau, *Mod. Phys. Lett. B* **3,** 93 (1989).
23. T. Manako, Y. Shimakawa, Y. Kubo, T. Satok, and Igarashi, *Physica C* **156,** 315 (1988).
24. S. Nakajima, M. Kikuchi, Y. Syono, N. Kobayashi, and Y. Muto, *Physica C* **168,** 57 (1990).
25. C. Michel, E. Suard, V. Caignaert, C. Martin, A. Maignan, M. Hervieu, and B. Raveau, *Physica C* **178,** 29 (1991).
26. J. P. Attfield and G. Férey, *J. Solid State Chem.* **80,** 112 (1989).
27. C. Martin, J. Provost, D. Bourgault, B. Domenges, C. Michel, M. Hervieu, and B. Raveau, *Physica C* **157,** 469 (1989).
28. A. Maignan, C. Martin, M. Hervieu, C. Michel, D. Groult, and B. Raveau, *Mod. Phys. Lett. B* **2**(5), 681 (1988).

29. M. O. KRAUSE AND J. H. OLIVER, *J. Phys. Chem. Ref. Data* **8,** 2 (1979).
30. A. BIANCONI, S. DELLA LONGA, C. LI, M. POMPA, A. CONGIU-CASTELLANO, D. UDRON, A. M. FLANK, AND P. LAGARDE, *Phys. Rev. B* 44(18), 10126 (1991).
31. A. BIANCONI *et al., Solid State Commun.* **63,** 1009 (1987).
32. H. TOLENTINO, A. FONTAINE, A. M. FLANK, P. LAGARDE, AND F. STUDER, *Physica C* **179,** 387 (1991).
33. H. ROMBERG, N. NÜCKER, M. ALEXANDER, J. FINK, D. HAHN, T. ZETTER, H. H. OTTO, AND K. F. RENK, *Phys. Rev. B* **41**(4), 2609 (1990).
34. R. M. HAZEN, "Physical Properties of High-Temperature Superconductors" (D. M. Ginsberg, Ed.), Vol. II, World Scientific, Teaneck, NJ (1990).